UNIVERSITÀ DEGLI STUDI DI TRIESTE
Dipartimento di
Scienze Chimiche e Farmaceutiche

Hybrid organic-gold nanoparticles for therapy and imaging

Prof. Lucia Pasquato

Second Conference Nano-Bio-Med-2013

ICTP, Trieste, 14th-18th October 2013

WHY GOLD?

- Au NPs of many different sizes (1-150 nm) can be fabricated in a controlled fashion with control over size dispersity and shape.
- the chemistry to protect the gold surface is well know
- a high density of ligands can be appended for targeting and/or drug-delivery.
- the monolayer can be modify with a variety of methodologies
- functional diversity can be readily achieved by creation of a multifunctional monolayer.
- the physical properties of the gold core may be exploited

➡ GNPs are ideal nanomaterials to serve as probes for investigating the influence of nanoparticle size, shape, and surface chemistry on their biological interactions.

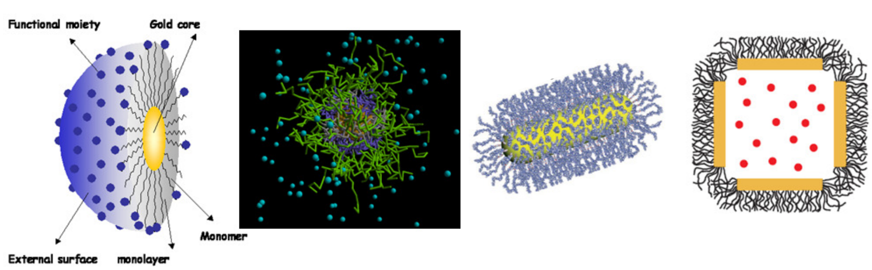

metal nanoparticles protected by a self-assembled organic layer

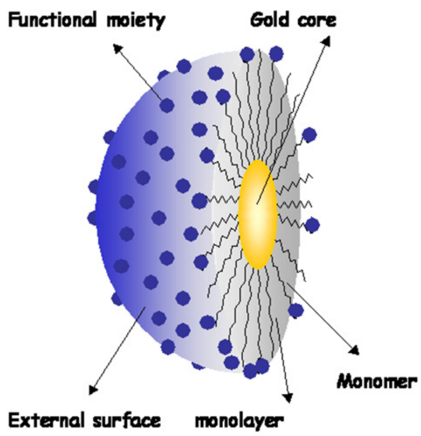

the metal core

✓ the size of the metal core determines the optical and elctronic properties

✓ the reaction conditions enable to tune the size, the shape and the dispersion

the self-assembled monolayer

✓ it is formed by a self-assembly process

✓ it is responsible for the stability
the solubility
the interaction with the environment
the function of the NP

GNPs for biomedical applications

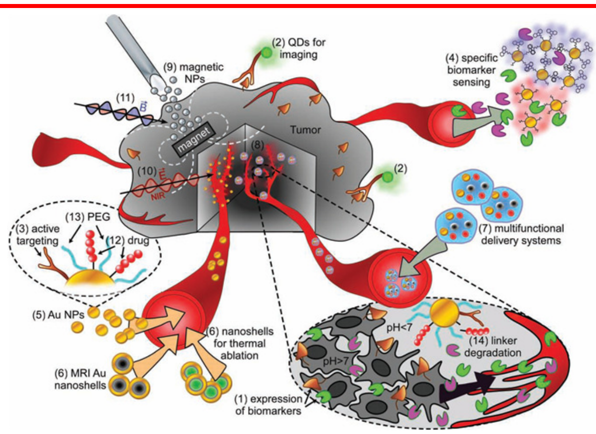

C. Minelli, S. B. Lowe, M. M. Stevens *Small* **2010**, *6*, 2336-2357.

Au NPs for **Imaging**
Au NPs for **Diagnosis**
Au NPs for **Therapy**

Gold NPs in Clinical trials

Phase I and Pharmacokinetic of CYT-6091

L. Tamarkin et al. *Clin. Cancer Res*. **2010**, *16*, 6139.

CYT-6091 – which is comprised of recombinant human tumor necrosis factor alpha (rhTNF)
Bound to the surface of PEGylated 27 nm colloidal gold particles
85% complete remission rates are routinely observed.
PEGylation of GNPs

- avoids immediate uptake by the reticuloendothelial reticulum (RES)
- Reduces the toxicity of rhTNF
- Allows the nanomedicine to sequester in solid tumors

  maximal antitumor responses were achieved at lower doses of drug.

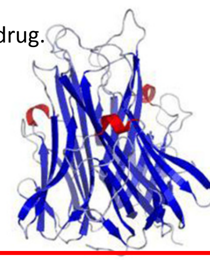

TNF-alpha is a homotrimer with a subunit molecular mass of 17 kDa

Gold NPs in Clinical trials

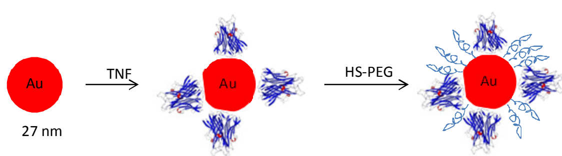

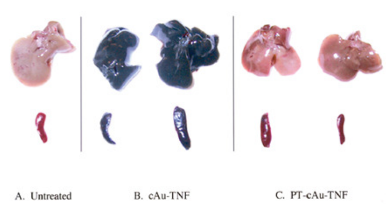

FIG. 2. Hepatic and splenic uptake of the cAu-TNF formulation and the PEG-THIOL cAu-TNF formulation (PT-cAu-TNF) compared to an untreated mouse. Two MC-38 tumor-burdened C57/BL6 mice were injected intravenously with the cAu-TNF vector, and another two tumor-burdened C57/BL6 mice were injected with the PT-cAu-TNF formulation. An untreated mouse and the four treated mice were sacrificed 5 hr after injection of 15 μg of the two different cAu formulations, and all five animals were perfused with heparinized saline. The livers and spleens from these animals were collected and photographed using a digitial camera. (a) Liver and spleen from an untreated mouse. (b) Livers and spleens from mice receiving the cAu-TNF vector. (c) Liver and spleen from mice receiving the PT-cAu-TNF vector.

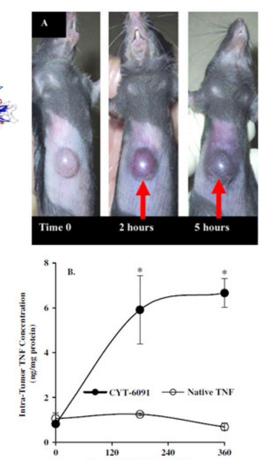

Fig. 3. A: Visual documentation of the accumulation of CYT-6091 (red arrows indicate location of the particle drug) in MC-38 tumors. **B:** Sequestration of CYT-6091 and TNF in MC-38-tumors. MC-38 tumor-burdened C57/BL6 mice were injected with 15μg of either native TNF or CYT-6091. TNF actively accumulates in the MC-38 tumors (*$P<0.05$ vs. native TNF Treatment and the time 0 point for CYT-6091 treatment). Reproduced from Paciotti et al., [2004], with permission of the publisher.

CytImmune is now collaborating with AstraZeneca to add a chemotherapeutic drug to further improve the killing power of CYT-6091.

Delivery

drug delivery via ‘active’ and ‘passive’ targeting

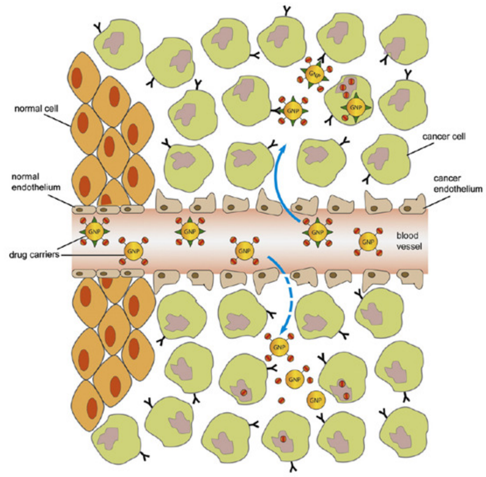

Delivery

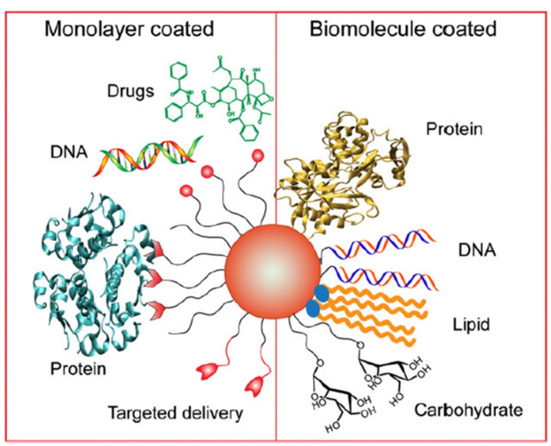

Schematic presentation of the two AuNP surface structures commonly employed in delivery applications.

multimodal drug delivery gold nanoparticles

- Prodrugs can be convalently conjugated to AuNPs via cleavable linkers.
- Hydrophobic drugs can be loaded onto AuNPs monolayer exploiting hydrophobic interactions, without structural modification of the drug payload.
- The release can be trigger by either internal (e.g. glutathione) or external (e.g. light) stimuli.

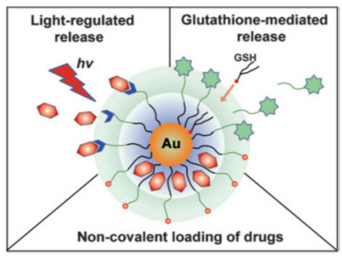

intracellurar GSH concentration 1-10 mM

Encapsulation or conjugation of therapeutic agents with NPs has proven to be a succesful approach

- to improving therapeutic's water solubility
- circulation time in the body
- uptake, in turn reducing drug payloads and associated toxic effects.

non-covalent loading

EPR Spectroscopy as a tool to investigate the monolayer properties

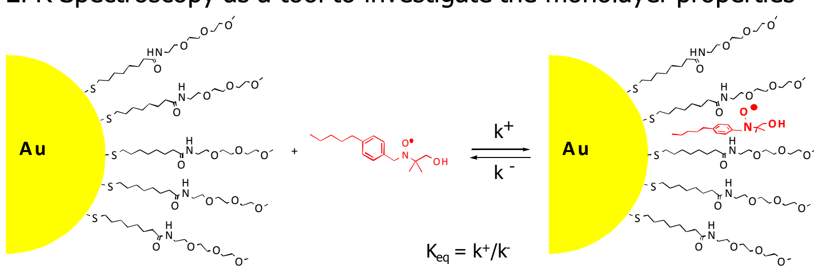

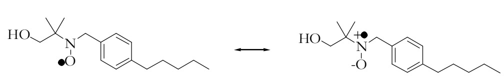

- the hyperfin coupling constants a(N) and $a(2H_{\beta})$ are larger in polar media

M. Lucarini, P. Franchi, G. F. Peduli, P. Pengo, P. Scrimin, L. Pasquato, *J. Am. Chem. Soc.*, **2004**, *126*, 9326.

non-covalent loading

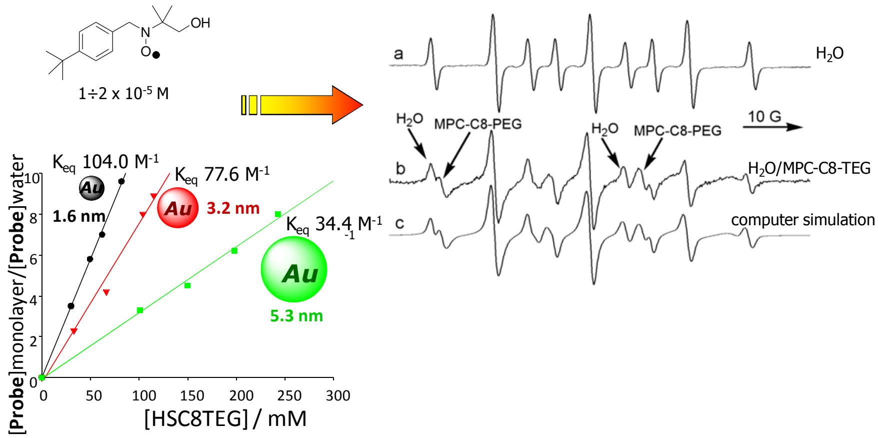

rapid exchange of the probe between the aqueous phase and the monolayer

the nitroxide group is located in a less polar environment shielded from the aqueous solvent

M. Lucarini, P. Franchi, G. F. Peduli, P. Pengo, P. Scrimin, L. Pasquato, *J. Am. Chem. Soc.*, **2004**, *126*, 9326.

non-covalent loading

Entrapment of Hydrophobic Drugs in Nanoparticle Monolayers with Efficient *Release into Cancer Cells*

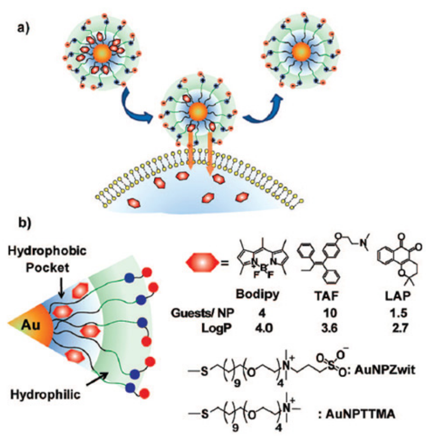

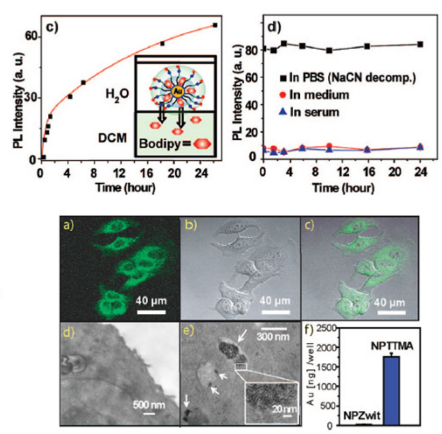

Figure 2. CLSM images of MCF-7 cell treated with **AuNPZwit-Bodipy** for 2 h: (a) green channel, (b) bright field, and (c) overlap. TEM images of fixed cell treated with (d) **AuNPZwit-Bodipy** and (e) **AuNPTTMA** as a positive control. Endosomally trapped AuNPs are marked by arrow. (f) ICP-MS measurement (200 000 cells/well), indicating low cellular uptake of **AuNPZwit** (31 ng/well after 4 h).

V. M. Rotello et al. JACS 2009, 131, 1360.

gold NPs for therapy and imaging

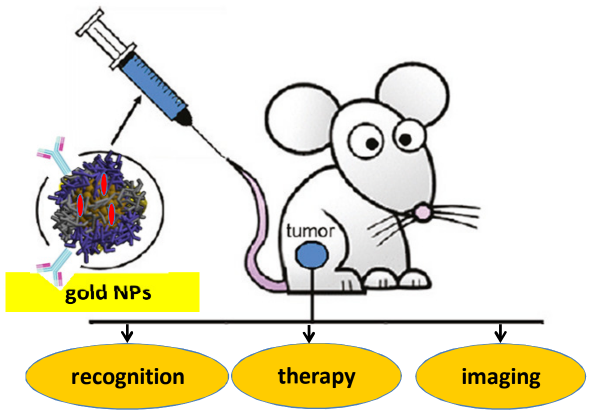

Effect of Surface Properties on NP–Cell Interactions

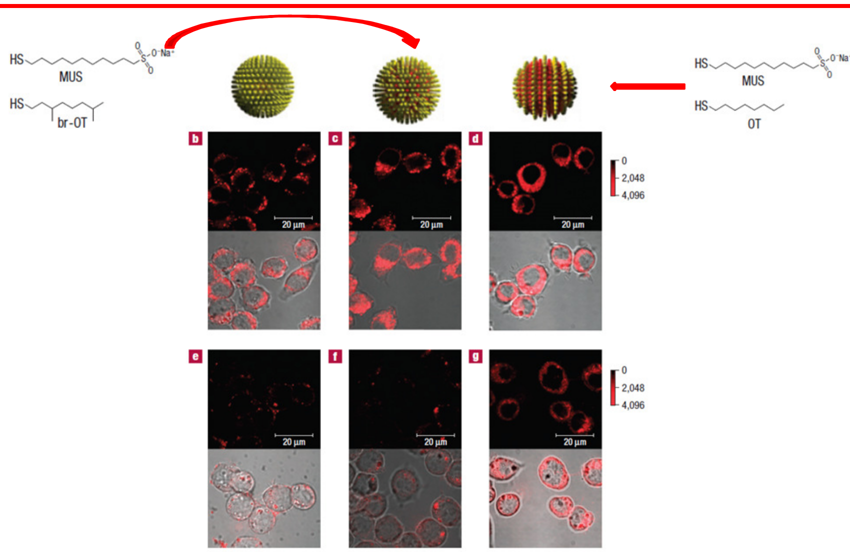

F. Stellacci et al. Nature Mat. 2008, 7, 588.

outline

gold nanoparticles protected by amphiphilic fluorinated ligands

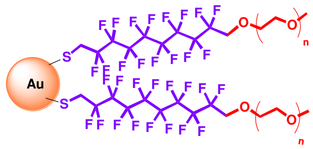

MPC-F8-PEG

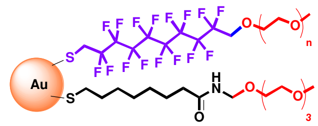

MPC-C8-TEG/F8-PEG

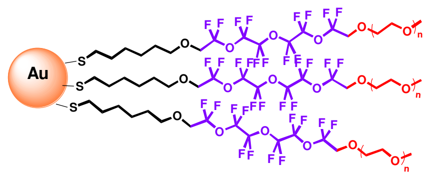

MPC-C6-FEO$_3$-PEG

NanoBioMed 2013, Triete, 14th-18th October

Comparison *F*- vs. *H*-alkyl chains

- (per)fluoroalkyl (*F*) chains are bulkier than alkyl (*H*) chains (cross section of ~ 30 Å^2 and 20 Å^2 respectively)
- they have a helical structure rather than a planar zig-zag structure
- monolayers of surfactants contaning *F*-chains are more stable than those formed from *H*-chains
- *F*-chains are amphiphobic (*i.e.*, at the same time hydrophobic and lipophobic) this difference promote self-aggregation
- short perfluoro chains are considered biocompatible and nontoxic
- fluoro-compounds are used for biomedical applications*, e.g.* as contrast agents for ^{19}F-MRI and ultrasonography, as drug delivery systems or as O_2 carriers.

van der Waals diameter 4.2 Å

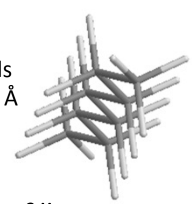

C_8H_{18}

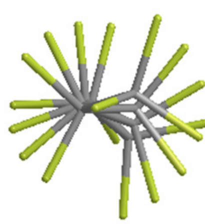

C_8F_{18}

van der Waals diameter 5.7 Å

NanoBioMed 2013, Triete, 14th-18th October

metal nanoparticles protected by fluorinated ligands

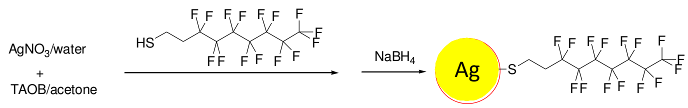

K. P. Johnston, B. A. Korgel et al. *JACS* **2000**, *122*, 4245.

dispersion in acetone and liquid and sc. CO_2

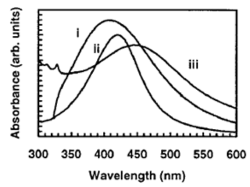

UV-visible absorbance spectra of AgNPs (i) coated with fluorinated ligands dispersed in acetone; (ii) coated with hydrocarbon ligands dispersed in hexane; (iii) coated with fluorinated ligands dispersed in sc-CO_2.

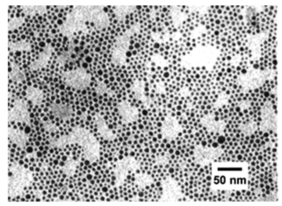

TEM image of silver nanocrystals coated with fluorinated ligands.

average size 5.5 nm

gold nanoparticles protected by fluorinated ligands

- use of commercially available *F*-thiols

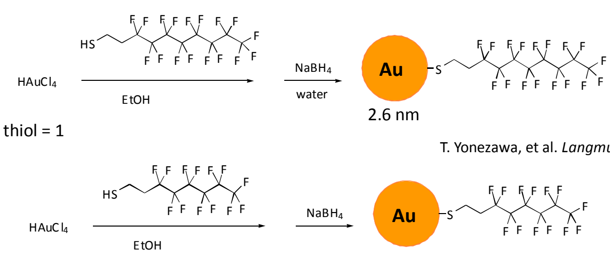

$Au_{545}SR_{108}$

2.6 nm

Au / thiol = 1

T. Yonezawa, et al. *Langmuir*, **2001**, *17*, 2291-2293.

2.4 nm

insoluble in common organic solvents: ethanol, acetone, chloroform, DMSO

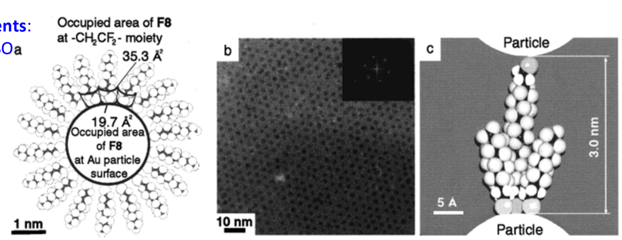

a dispersion in HCFC-225 dropcasted on a carbon-coated copper grid displays ordered hexagonal assembly

gold nanoparticles protected by fluorinated ligands

- synthesis by ligand exchange

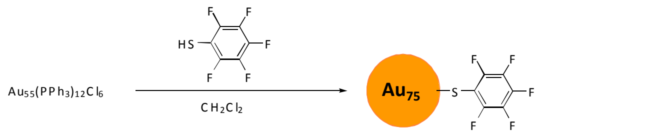

~ 1.4 nm

soluble in CH_2Cl_2, THF, DMF

- synthesis by Brust reaction

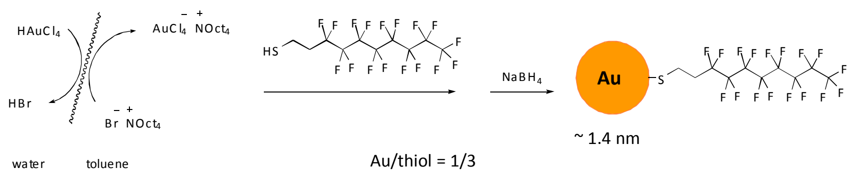

~ 1.4 nm

Au/thiol = 1/3

AuNPs soluble in non polar fluorinated solvents only

A. Dass, R. Guo, J. B. Tracy, R. Balasubramanian, A. D. Douglas, R. W. Murray *Langmuir*, **2008**, *24*, 310-315.

- Au/thiol = 3/1 averge core diameter 2.5 nm; J. Im, A. Chandekar, J. E. Whitten *Langmuir*, **2009**, *25*, 4288-4292.

NanoBioMed 2013, Triete, 14th-18th October

gold nanoparticles protected by fluorinated ligands

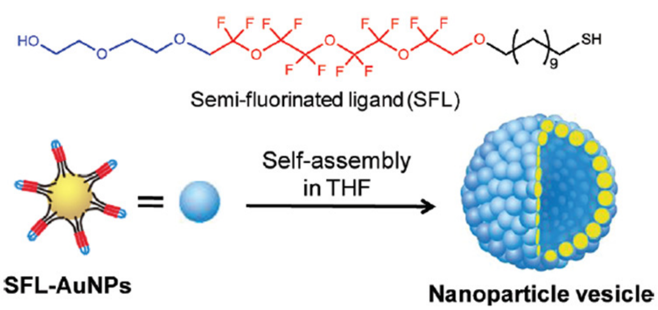

5, 10, 20 nm

the solvophobic feature of the fluorinated bundles is the driving force for NP assembly

K. Niikura *et al. J. Am. Chem. Soc.* **2012**, *134*, 7632.

NanoBioMed 2013, Triete, 14th-18th October

gold nanoparticles protected by amphiphilic fluorinated ligands

Synthesis

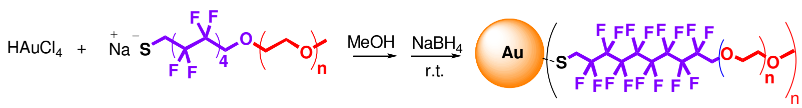

n = 3
n = 4
n = 6
n = 12,13 **MPC-F8-PEG**

- RSH/Au molar ratio = 2
- reaction at r.t. to favor RSH solubility
- for n= 3, 4 and 6 NPs precipitate in MeOH, they are scarcely soluble in DCM and chloroform

C. Gentilini, F. Evangelista, P. Rudolf, P. Franchi, M. Lucarini, L. Pasquato *J. Am. Chem. Soc.* **2008**, *130*, 15678-15682.

NanoBioMed 2013, Triete, 14th-18th October

gold nanoparticles protected by amphiphilic fluorinated ligands

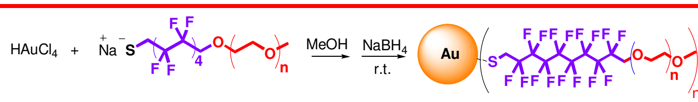

n = 12-13

MPC-F8-PEG

RSH/Au	NP core average diameter (nm)
0.7	2.9
2	2.7
2.5	1.6

average composition: $Au_{670}(SF8PEG)_{107}$

✓ NPs are soluble in water, methanol, DCM and chloroform

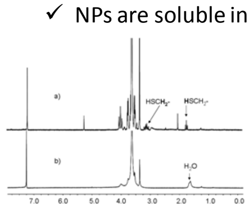

(a) [1]H NMR of HS-F8-PEG and (b) [1]H NMR of MPC-F8-PEG prepared with a thiol/Au ratio of 2:1.

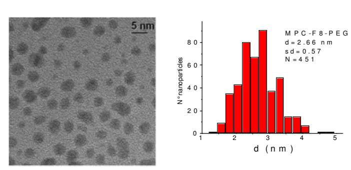

TEM image and histogram of MPC-F8-PEG.

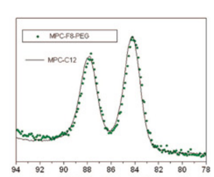

XPS Au 4f core level spectra of MPC-F8-PEG and MPC-C12.

NanoBioMed 2013, Triete, 14th-18th October

gold nanoparticles protected by amphiphilic fluorinated ligands

radical probe

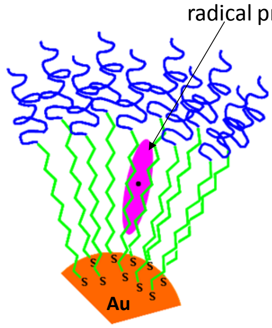

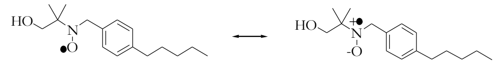

radical probe

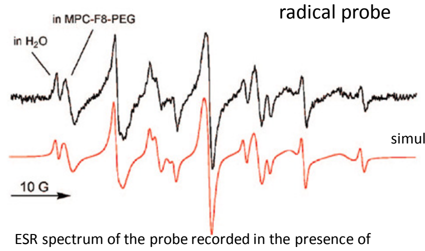

perfluorinated alkyl chain
poly(oxoethylene) chain

ESR spectrum of the probe recorded in the presence of MPC-F8-PEG 0.56 mM (in black) and the corresponding computer simulation (in red).

ESR parameters of the radical probe (1 G = 0.1 mT) and partition equilibrium (Keq) constants at 298 K.

	a(N)/G	$a(2H_\beta)$/G	g-factor	K_{eq} / M^{-1}
water[a]	16.25	10.14	2.0056	—
MPC-F8-PEG	15.46	8.68	2.0057	176
MPC-C8-TEG[b]	15.67	8.97	2.0057	87[c]

[a] Contains 10% (v/v) of methanol. [b]From reference 27. [c] See reference 33.

C. Gentilini, F. Evangelista, P. Rudolf, P. Franchi, M. Lucarini, L. Pasquato *J. Am. Chem. Soc.* **2008**, *130*, 15678-15682.

phase segregation of hydrogenated/fluorinated units

block terpolymer

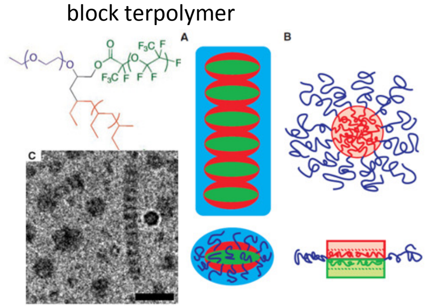

T. P. Lodge et al. *Science* **2004**, *306*, 98

Liposomes

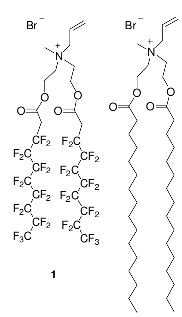

1

2

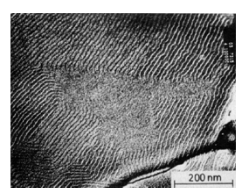

monolayers

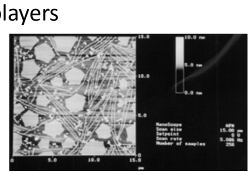

AFM images of a mixed monolayer of 1:1 $C_{18}H_{37}SO_3Na$–$C_8F_{17}COOH$ deposited on a freshly cleaved mica surface at a compression rate of 35 cm^2 min^{-1}. *Coll. Surf. A*, **1999**, *157*, 63–71.

Freeze fracture electron micrograph of a phase-separated liposomal membrane (95 mol % **DMPC** and 5 mol % fluorinated lipid **3**. The ripple structure shows the parts of membrane composed of DMPC, surrounding a domain of the fluorinated lipid (smooth surface). R. Elbert, T. Folda, and H. Ringsdorf *J. Am. Chem. Soc.* **1984**, *106*, 7687-1692

gold nanoparticles protected by *H-/F-* mixed-monolayers

- Homogeneous phase synthesis (methanol/water) using mixtures of thiolates with **immiscible chains**

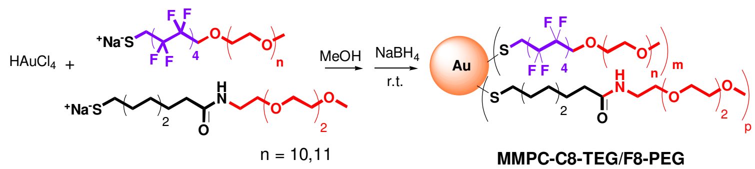

- synthesis of mixed-monolayer by exchange reaction

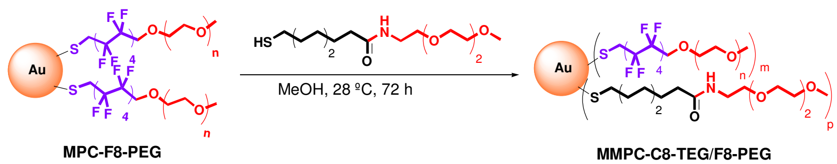

C. Gentilini, P. Franchi, E. Mileo, S. Polizzi, M. Lucarini, L. Pasquato *Angew. Chem. Int. Ed.* **2009**, *48*, 3060.

gold nanoparticles protected by *H-/F-* mixed-monolayers

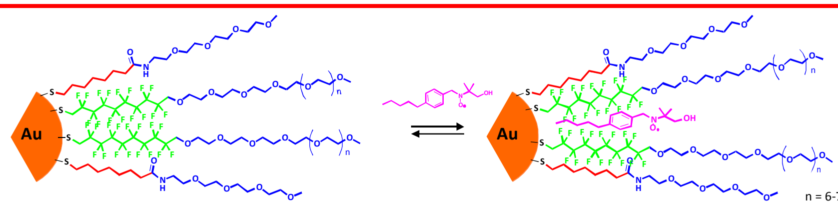

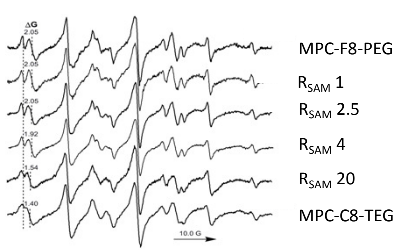

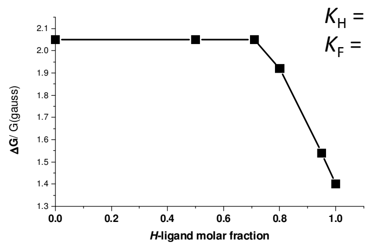

K_H = 104 M^{-1}
K_F = 176 M^{-1}

C. Gentilini, P. Franchi, E. Mileo, S. Polizzi, M. Lucarini, L. Pasquato *Angew. Chem. Int. Ed.* **2009**, *48*, 3060.

gold nanoparticles protected by *H-/F-* mixed-monolayers

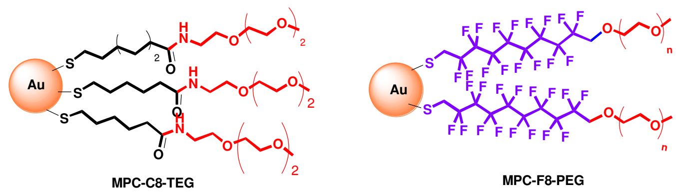

MPC-C8-TEG MPC-F8-PEG

ESR Parameters in the Presence of Homoligand NP Mixtures

χ	$\Delta G/G$	
0	2.05	2.05
0.5	2.05	1.90
0.71	2.05	1.84
0.80	1.92	1.68
0.95	1.54	1.50
1	1.40	1.45

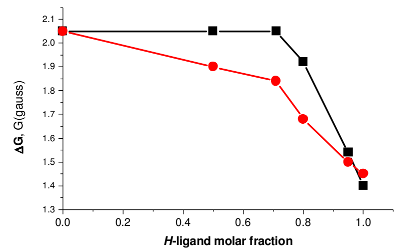

P. Posocco, C. Gentilini, S. Bidoggia, A. Pace, P. Franchi, M. Lucarini, M. Fermeglia, S. Pricl, L. Pasquato, *ACS Nano* **2012**, *6*, 7243-7253.

gold nanoparticles protected by *H-/F-* mixed-monolayers

$$\Delta G = 1.40X_H + 2.05(1 - X_H)$$

$$X_H = \frac{\dfrac{K_H[\textbf{\textit{H}}\text{-ligand}]}{K_F[\textbf{\textit{F}}\text{-ligand}]}}{1 + \dfrac{K_H[\textbf{\textit{H}}\text{-ligand}]}{K_F[\textbf{\textit{F}}\text{-ligand}]}}$$

K_H = 104 M^{-1}
K_F = 176 M^{-1}

χ	$\Delta G/G$ HeteroL	HomoL	calcd.
0	2.05	2.05	2.05
0.5	2.05	1.90	1.82
0.71	2.05	1.84	1.69
0.80	1.92	1.68	1.60
0.95	1.54	1.50	1.45
1	1.40	1.45	1.40

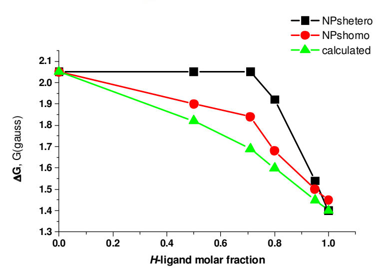

L. Pasquato et al., *ACS Nano* **2012**, *6*, 7243-7253.

gold nanoparticles protected by *H-/F-* mixed-monolayers

atomistic and mesoscale calculations

- Models of the NPs were obtained employing an innovative **multiscale molecular simulation** approach
- This approach combines **mesoscale techniques**, developed to describe systems with properties at the nanometer scale, and **atomistic techniques**, which model matter at the level of atoms
- In particular, morphological characterization of the NPs was predicted using mesoscale models (*Dissipative Particle Dynamics*), whose chemical potentials were derived from simulations at a lower level of detail (*Molecular Dynamics*)
- Simulation have been carried out in the presence of water as solvent, at 298 K, and considering the mobility of the thiolates on the gold surface

L. Pasquato et al., *ACS Nano* **2012**, *6*, 7243-7253.

gold nanoparticles protected by *H-/F-* mixed-monolayers

Ligand organization on the surface of gold NPs at different molar fraction of the two ligands

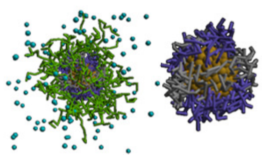

χ_H = 0.50, ∅ 2.2 nm

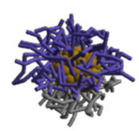

χ_H = 0.50, ∅ 1.6 nm

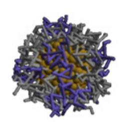

χ_H = 0.71, ∅ 2.5 nm

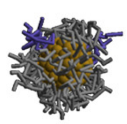

χ_H = 0.80, ∅ 1.9 nm

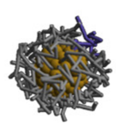

χ_H = 0.95, ∅ 1.9 nm

P. Posocco, C. Gentilini, S. Bidoggia, A. Pace, P. Franchi, M. Lucarini, M. Fermeglia, S. Pricl, L. Pasquato, *ACS Nano* **2012**, *6*, 7243-7253.

NanoBioMed 2013, Triete, 14th-18th October

gold nanoparticles protected by *H-/F-* mixed-monolayers

Equilibrium constants (T = 298 K) in the presence of Heteroligand mixed-monolayers

χ	K_{mix}/M^{-1}	K_H/K_F [e]	K_F/M^{-1}	K_H/M^{-1}
0	176 [a]		176 [a]	
0.50	100 ± 7.7 [b]	<0.04	200	<10
0.71	100 ± 8.1	<0.04	350	<10
0.80	189 ± 20	0.06	762 [f]	45 [f]
0.95	120 ± 11	0.16	600 [f]	96 [f]
1	104 [c]			104 [c]

shell thickness F8PEG 2.82 nm in homoligand NPs
C8TEG 1.40 nm

F8PEG 2.60 nm in heteroligand NPs
C8TEG 1.59 nm

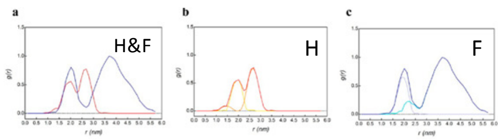

Radial distribution functions (RDFs) for the SAM components of MPC-C8-TEG/F8-PEG, 1:1

it is apparent that the small ligand chains somewhat stretch out toward the longer ones and these in turn bend over the smaller counterpart.

L. Pasquato et al., *ACS Nano* **2012**, *6*, 7243-7253.

gold nanoparticles protected by *H-/F-* mixed-monolayers

conclusions

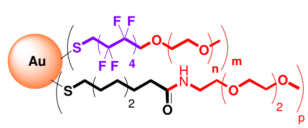

Phase segregation occurs for all molar fractions considered, even when about three **F**-chains (4%) are present in the monolayer.

The shape of the domains is triggered by:

- the **relative length of the ligands** as the consequence of the optimum balance between enthalpic and entropic force.
- the **size of the NP core** : below 2 nm Janus domains are formed, whereas stripes-like domains spontaneously form for larger NPs.
- the composition of the mixed-monolayer

mixtures of *H*-ligands and *F*-ligands of different length are ideal to control the morphology of mixed self-assembled monolayers in three dimensions.

mixed-monolayers present features that are different from those of the parent homoligand monolayers.

L. Pasquato et al., *ACS Nano* **2012**, *6*, 7243-7253.

NanoBioMed 2013, Triete, 14th-18th October

MAGNETIC RESONANCE IMAGING

- MRI is a particular attractive imaging modality for clinical trials.
  - it provides high-resolution,
  - detailed structural images,
  - three-dimensional spatial reconstruction,
  - no ionizing radiation
- It can be used for:
  - disease detection
  - therapeutic monitoring
  - treatment efficacy
  - cell tracking

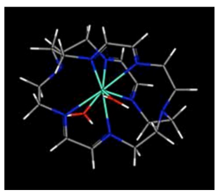

- ^{1}H MRI
- Gadolinium-based contrast agents (GBCAs)

- SuperParamagnetic Iron Oxide (SPIO) NPs
- 50 – 180 nm
- USPIO , 10-50 nm
- VSPIO, < 10 nm
-

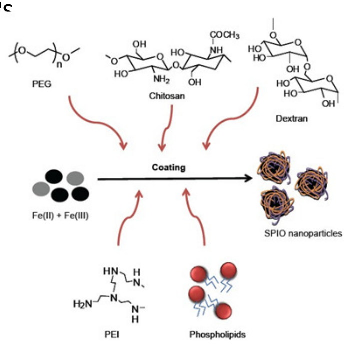

Feridex, Resovist

Clinically approved
Rapidly removed

- ^{19}F MRI

^{19}F MRI

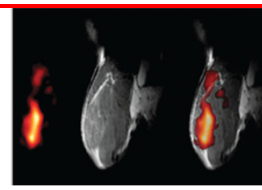

Nat. Biotechnol. **2005** *23*,983.

- high relative sensitivity (83% of ^{1}H)
- 100% natural abundance of ^{19}F
- its resonance differs by only 6% from that of ^{1}H
- an extremely broad range (> 200 ppm) which permits unambiguous identification of distinctive ^{19}F-containing compounds, but sensitive to the environment
- tissues have a negligible background ^{19}F signal, quantitative analysis are allowed
- perfluorocarbons (PFCs) have been extensively studied for biomedical applications.
- a very high ***F*** concentration is needed

Ruiz-Cabello, J.; Barnetta, B. P.; Bottomleya, P. A.; Bulte, J. W. M. *NMR Biomed.* **2011**, *24*, 114–129.
Srinivas, M.; Heerschap, A.; Ahrens, E.T.; Figdor, C. G.; de Vries, I. J. M. *Trends Biotech.* **2010**, *28*, 363-370.

^{19}F MRI

PFCs

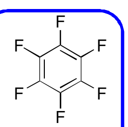

PFB

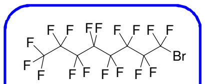

PFOB

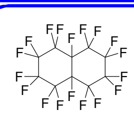

Perfluorodecalin

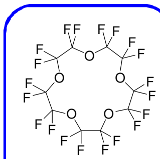

15-crown-5-ether

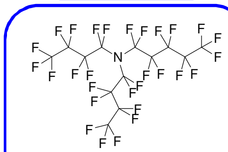

Oxypherol ™
PFTA

Perfluoroether nanoemulsion

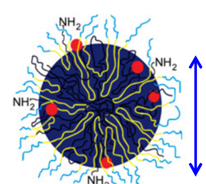

160-190 nm

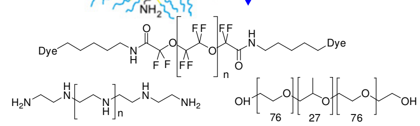

Dual ^{19}F MRI-fluroescence detection

Ahrens, E. T.; Janjic, J. M.; Srinivas, M.; Kadayakkara, D. K. K. *J. Am. Chem. Soc.* **2008**, *130*, 2831-2841.

GNPs for ^{19}F MRI

design, synthesis and use of gold NPs protectected by fluorinated ligands as nanomaterial for imaging and therapy

modular system

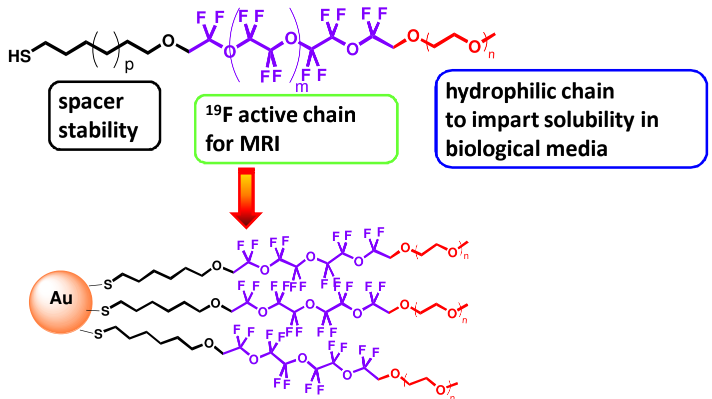

L. Pasquato et al. *Chem. Commun.* **2013**, *49*, 8794.

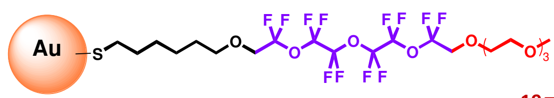

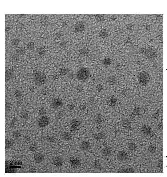

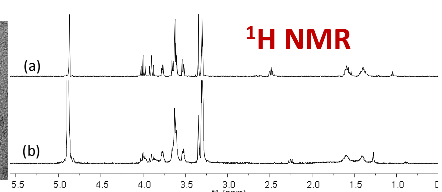

^{1}H NMR (500 MHz, CD_3OD) of thiol (a) and MPC C6-OF-EG3 (b).

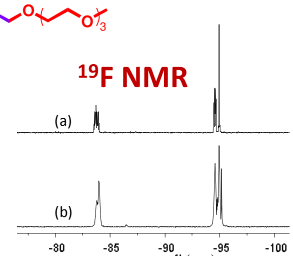

^{19}F NMR (500 MHz, CD_3OD) of protected thiol (a) and MPC C6-OF-EG3 (b).

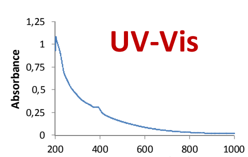

UV-Vis spectrum in methanol.

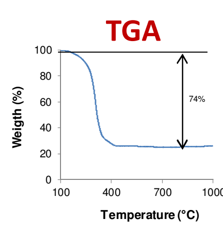

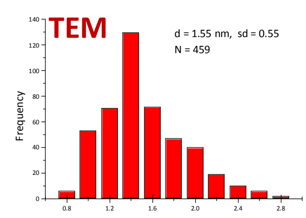

MPC-C6-FEO-EG3, ^{19}F MRI

40 mg/mL of NP (1.75×10^{20} ^{19}F/mL)

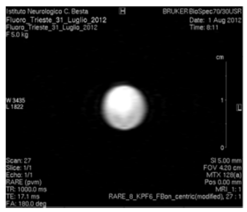

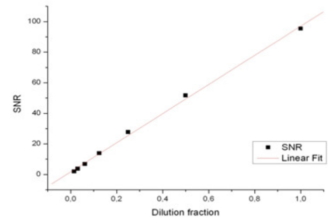

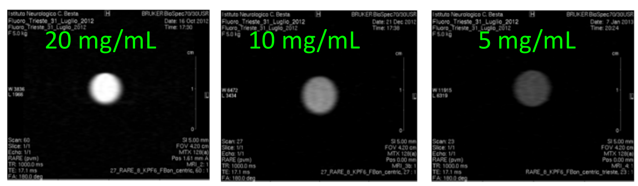

I. Zucca, Institute C. Besta, Milan

MPC-C6-FEO-EG3

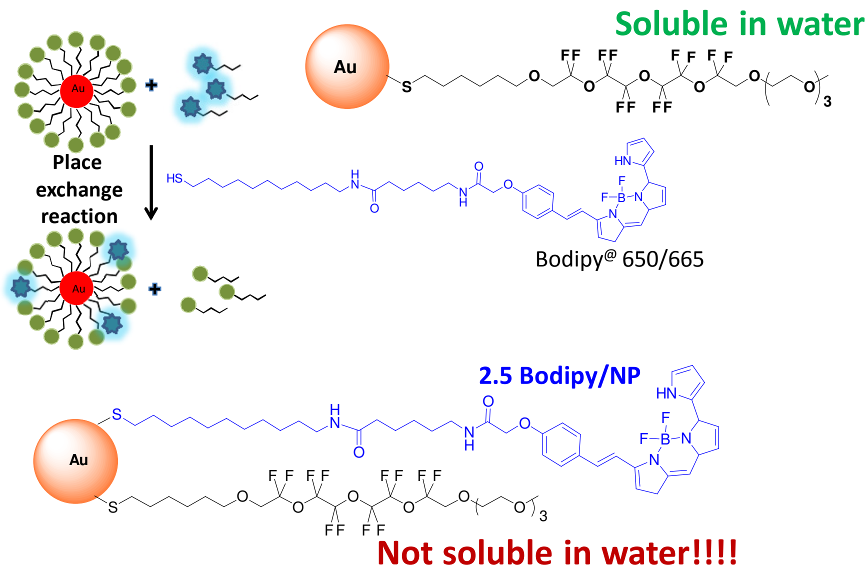

MPC-C6-FEO-PEG

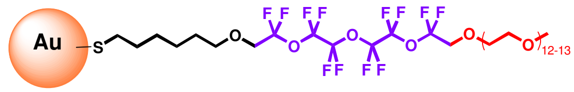

^{1}H NMR

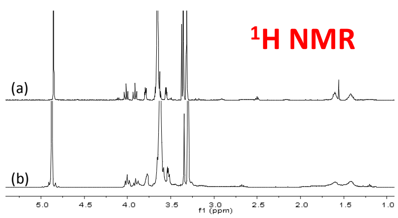

^{1}H NMR (500 MHz, CD_3OD) of thiol (a) and MPC C6-OF-PEG (b).

^{19}F NMR

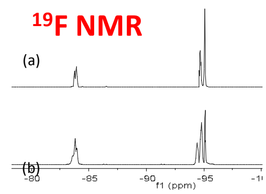

^{19}F NMR (500 MHz, CD_3OD) of protected thiol (a) and MPC C6-OF-PEG (b).

UV-Vis

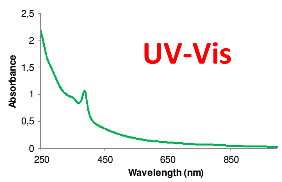

UV-Vis spectrum in methanol.

TGA

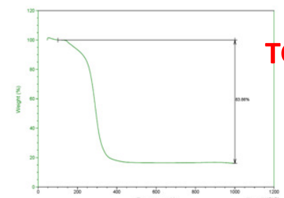

MPC-C6-FEO-PEG

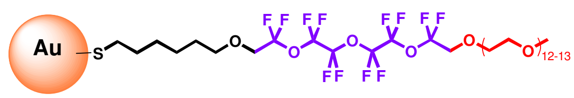

TEM

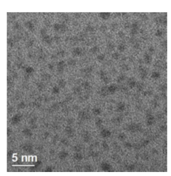

STEM-HAADF

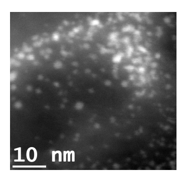

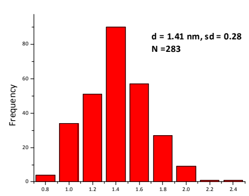

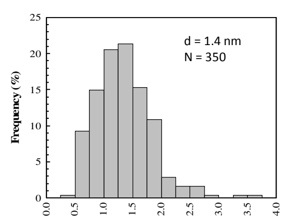

Juan J. Delgado, Univ. de Cádiz, Spain

MPC-C6-FEO-PEG

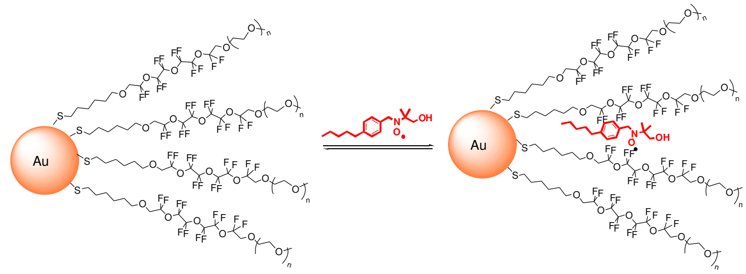

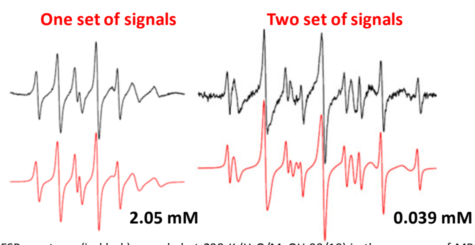

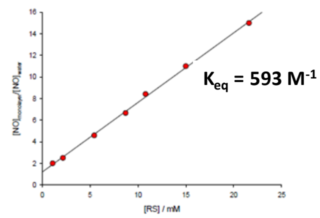

ESR spectrum (in black) recorded at 298 K (H_2O/MeOH 90/10) in the presence of MPC C6-OF-PEG 2.05 mM ([RS] = 109 mM) (left) and of MPC C6-OF-PEG 0.039 mM ([RS] = 2.17 mM) (right) and the corresponding computer simulation (in red).

M. Lucarini, P. Franchi, Univ. Bologna

Plot of the ratio between the concentration of the probe partioned in the monolayer and that of the free species as a function of ligand concentration bound to gold.

gold nanoparticles protected by amphiphilic fluorinated ligands

	a(N)/G	a(2H$_\beta$)/G	g-factor	d core	K_{eq}/M^{-1}
Water	16.25	10.14	2.0056	-	-
MPC C8-TEG	15.67	8.97	2.0057	1.4 nm	110*
MPC F8-PEG	15.46	8.68	2.0057	2.7 nm	176
MPC C6-OF-PEG	**15.45**	**8.65**	**2.0057**	**1.4 nm**	**593**

*calculated

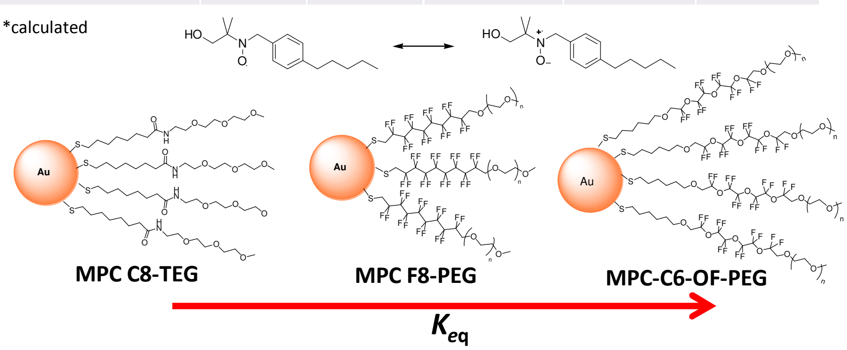

MPC-C6-FEO-PEG

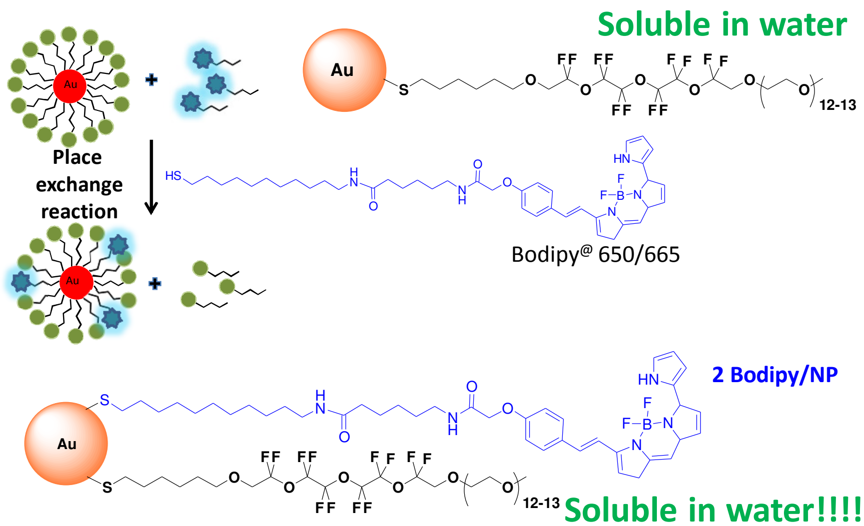

MPC-C6-FEO-PEG, cellular uptake

4 h incubation with HeLa cells at 37 ºC, and 30 min RBC

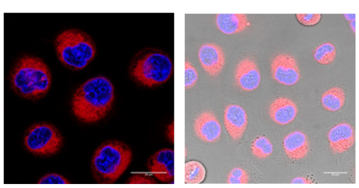

Confocal laser microscopy images of HeLa cells (nucleus stained in blue, Hoechst dye) loaded with F-MPCs **4b** (red fluorescent signal) for 4 h at 37 °C.

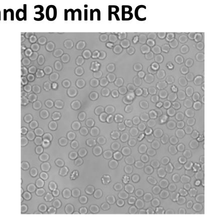

RBCs do not uptake NPs only free dye is able to penetrate their cell membrane or remain attached to the membrane.

No unbound Bodipy was detected by RBC test.

4 h incubation with HeLa cells at 4 ºC (endocytic/ pinocytic mechanisms are arrested)

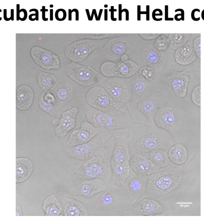

No visible red signal, only very little is possible visualized with the enhanced signal.

F. Sousa, IEO, Milan

MPC-C6-FEO-PEG, cellular viability

UL – dead cells not labeled with NPs
UR - dead cells labeled with NPs
LL – viable cells not labeled with NPs
LR- viable cells labeled with NPs

FACS for PI of HeLa incubated 4 hrs with MPC C6-FEO-PEG

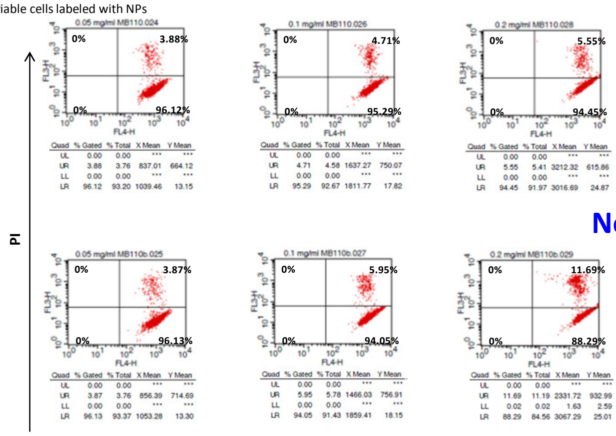

0.05 mg/ml MB110.024

Quad	% Gated	% Total	X Mean	Y Mean
UL	0.00	0.00	***	***
UR	3.88	3.76	837.01	664.12
LL	0.00	0.00	***	***
LR	96.12	93.20	1039.46	13.15

0.1 mg/ml MB110.026

Quad	% Gated	% Total	X Mean	Y Mean
UL	0.00	0.00	***	***
UR	4.71	4.58	1637.27	750.07
LL	0.00	0.00	***	***
LR	95.29	92.67	1811.77	17.82

0.2 mg/ml MB110.028

Quad	% Gated	% Total	X Mean	Y Mean
UL	0.00	0.00	***	***
UR	5.55	5.41	3212.32	615.86
LL	0.00	0.00	***	***
LR	94.45	91.97	3016.69	24.87

No cytotoxicity

0.05 mg/ml MB110b.025

Quad	% Gated	% Total	X Mean	Y Mean
UL	0.00	0.00	***	***
UR	3.87	3.76	856.39	714.69
LL	0.00	0.00	***	***
LR	96.13	93.37	1053.28	13.30

0.1 mg/ml MB110b.027

Quad	% Gated	% Total	X Mean	Y Mean
UL	0.00	0.00	***	***
UR	5.95	5.78	1466.03	756.91
LL	0.00	0.00	***	***
LR	94.05	91.43	1859.41	18.15

0.2 mg/ml MB110b.029

Quad	% Gated	% Total	X Mean	Y Mean
UL	0.00	0.00	***	***
UR	11.69	11.19	2331.72	932.99
LL	0.02	0.02	1.63	2.59
LR	88.29	84.56	3067.29	25.01

The percentage of viable cells is above **95%** after taken up NPs. The percentage of dead cells labeled with NPs are very similar to all concentrations tested.

GNPs for ^{19}F MRI

NMR/MRI

Relaxation times (^{19}F-NMR)

T1 (spin-lattice relaxation time)

Inversion Recovery

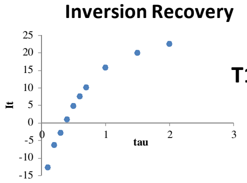

T1 = 588 ms

T2 (spin-spin relaxation time)

CPMG sequence

(Carr-Purcell Meiboom-Gill)

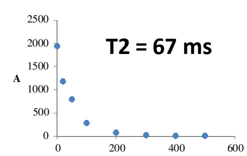

T2 = 67 ms

^{19}F-MR images

18.75mg/mL of NPs (6.06×10^{19} ^{19}F/mL)

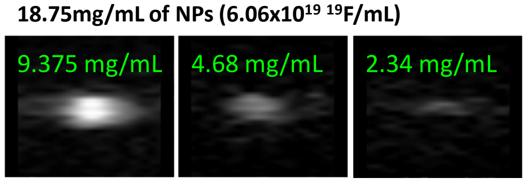

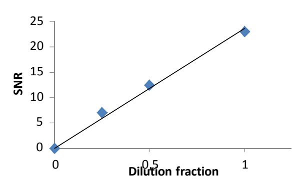

L. Pasquato et al. *Chem. Commun.* **2013**, *49*, 8794.

Concluding remarks

✓ Amphiphilic *F*-ligands have been used succesfully in the passivation of gold NPs whic become very stable and soluble in organic solvents and in water

✓ *F*-ligands when in the monolayer become interesting tools to introduce new features and the properties of F nucleous

✓ mixtures of *F*- and *H*-ligands enable to control the morphology of mixed-monolayers graphted on spherical gold surfaces.
Moreover, they show phase segregation independently on the monolayer composition. This behaviour may favor multivalent recognition and cooperative catalysis processes

✓ The properties of mixed-monolayers are different from those of the parent homoligand monolayers

✓ Gold NPs coated with fluorinated ligands present features suitable for ^{19}F MRI
✓ These monolayers may be used on NP of different materials

ACKNOWLEDGEMENTS

Università di Trieste, DSCF
Paolo Pengo
Cristina Gentilini
Mariangela Boccalon
Silvia Bidoggia
Alice Pace
Maria Vintila

Sabrina Pricl **(DIA)**
Paola Posocco
Maurizio Fermeglia

EPFL Lausanne, CH
Francesco Stellacci
Randy Carney

Università di Firenze
Cristina Nativi
Barbara Richichi

IFOM, Milano
Fernanda Sousa

University of Cadiz
Jan Jousé Delgado

Università di Padova
Paolo Scrimin
Fabrizio Mancin
Paolo Pengo

Università di Bologna
Marco Lucarini
Gian Franco Pedulli
Paola Franchi
Elisabetta Mileo

University of Venezia
Stefano Polizzi
Patrizia Canton

University of Groningen
Petra Rudolf
Fabrizio Evangelista

BESTA Neurological Institute, Milano
Roberto Spreafico
Ileana Zucca

MIUR, INSTM, Regione FVG, Ministero della Salute, UNITS